Supporting Information

Tailored template engineering of $MoSe_2$/N, P-doped carbon nanospheres with sandwiched carbon and few-layered $MoSe_2$ shells for stable and high-rate storage of Na^+/K^+-ions

Xiaotong Wang,[a] Wenpei Kang,*[b] Yuyu Wang,[a] Bingchen Zhang[b] and Daofeng Sun*[b] a. College of Science, China University of Petroleum (East China), Qingdao 266580, PR China

b. School of Materials Science and Engineering, China University of Petroleum (East China), Qingdao 266580, PR China

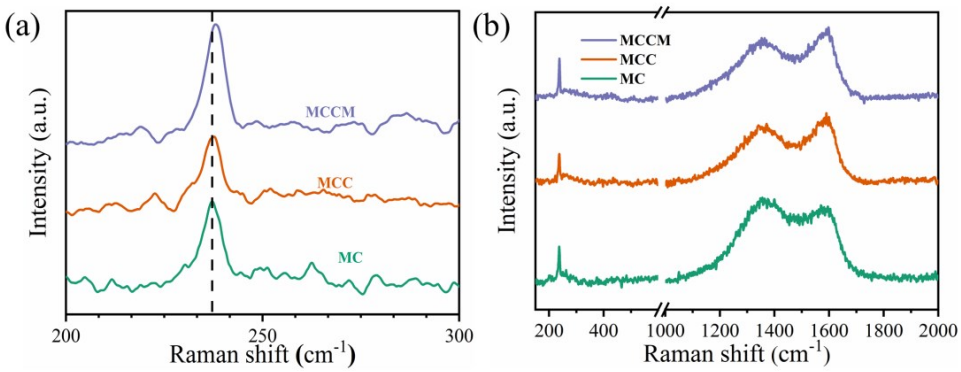

Fig. S1. (a) magnified and (b) integral Raman spectra for MC, MCC and MCCM anodes.

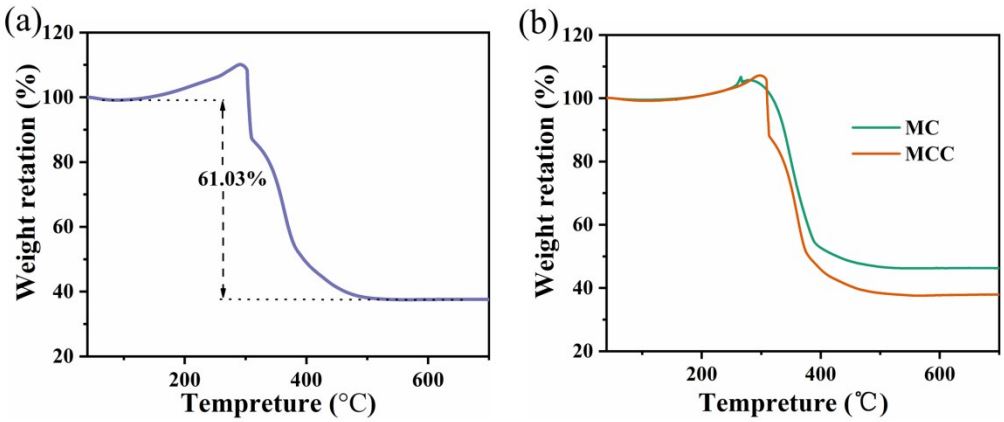

Fig. S2. TGA curves of (a) MCCM and (b) MC and MCC samples from room temperature to 700 °C in an O_2 atmosphere.

Through the TGA analysis, the carbon content can be obtained. And the calculating process is as following.

Take MCCM as an example, we assume the mole ratio of C: Mo = n. During the TGA test in O_2 atmosphere, the corresponding oxidation reactions is as follows.

$$MoSe_2/N,P\text{-}C@N\text{-}C \subset MoSe_2 + O_2 \rightarrow MoO_3 + CO_2$$

$$254+ 12n \qquad\qquad 144 \qquad 44n$$

From this reaction, the weight loss ratio after calcination in O_2 atmosphere is as follows.

$$\frac{254 + 12n - 144}{254 + 12n}$$

Based on the weight loss of 61.03% measured from TGA, an equation can be given:

$$\frac{254 + 12n - 144}{254 + 12n} = 61.03\%$$

$$n = 9.626$$

So the carbon content in MCCM is determined to be 31.25% ($\frac{12 \times 9.626}{254 + 12 \times 9.626}$). And the carbon contents of MC and MCC can be obtained through the same calculation process, based on their weight losses, giving 53.26% and 61.85%, respectively.

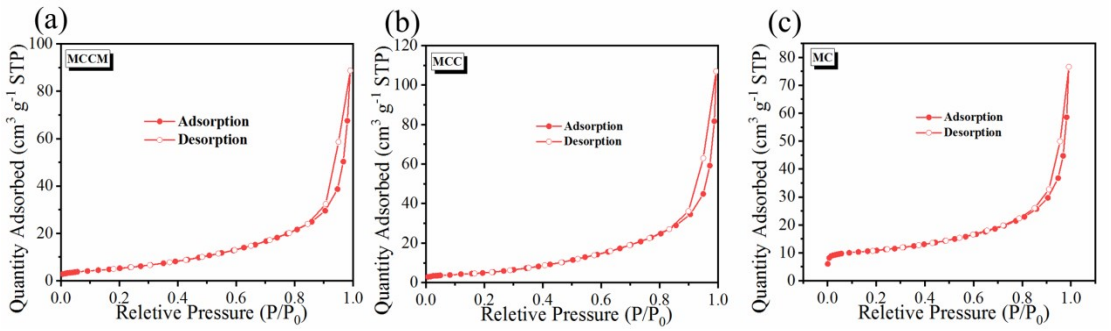

Fig. S3. N_2 adsorption-desorption isotherms curves of (a) MCCM, (b)MCC and (c) MC.

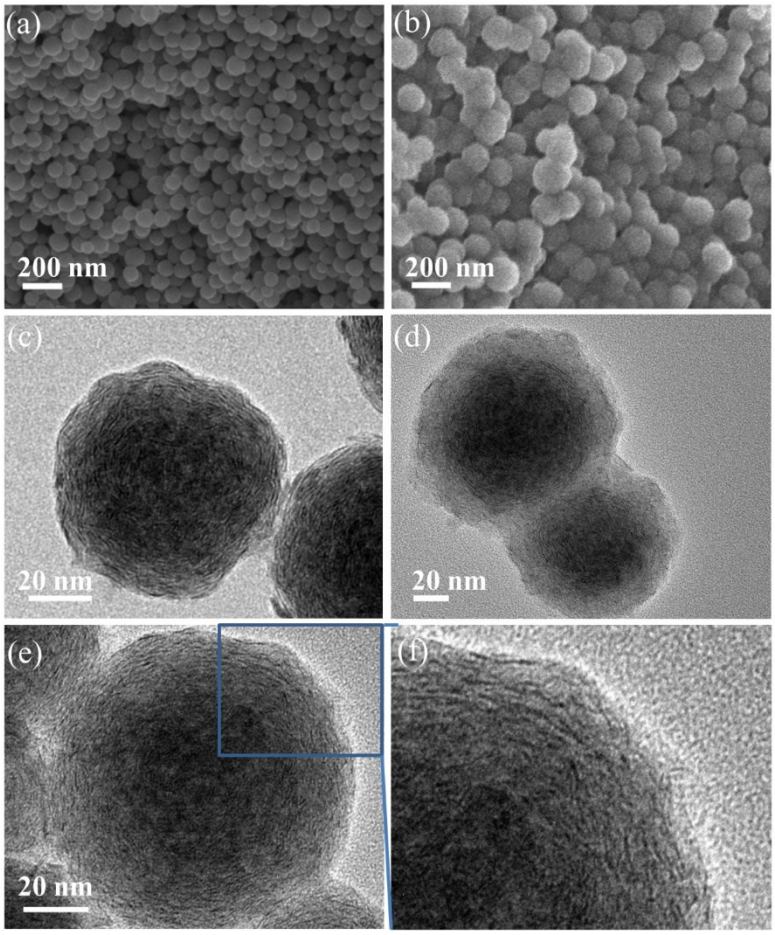

Fig. S4. SEM images of (a) PPy-PMo_{12} and (b) PPy-PMo_{12}-PDA; TEM images of (c) MC and (d-f)

MCC.

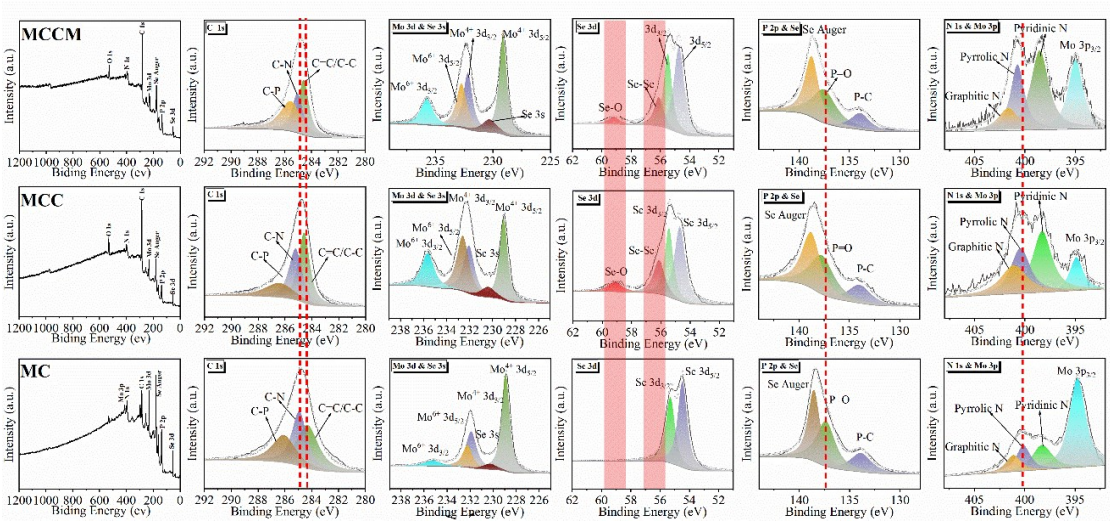

Fig. S5. Comparison of the XPS spectra for the MCCM, MCC and MC.

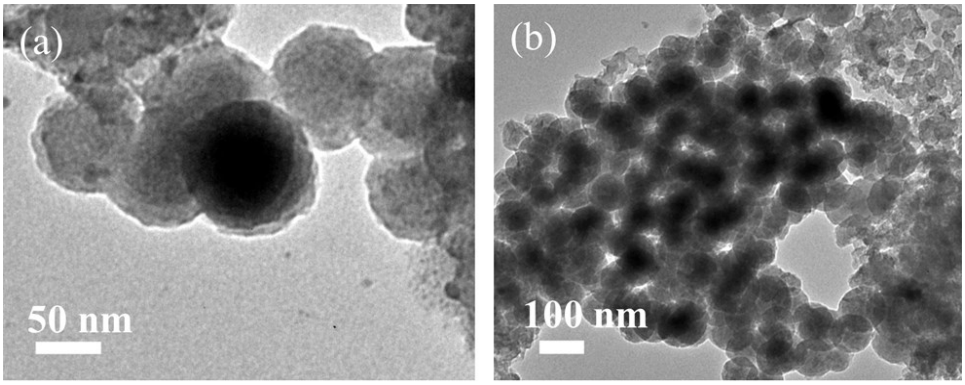

Fig. S6.TEM images of MCCM after discharge/charge cycling in (a)SIBs and (b) PIBs.

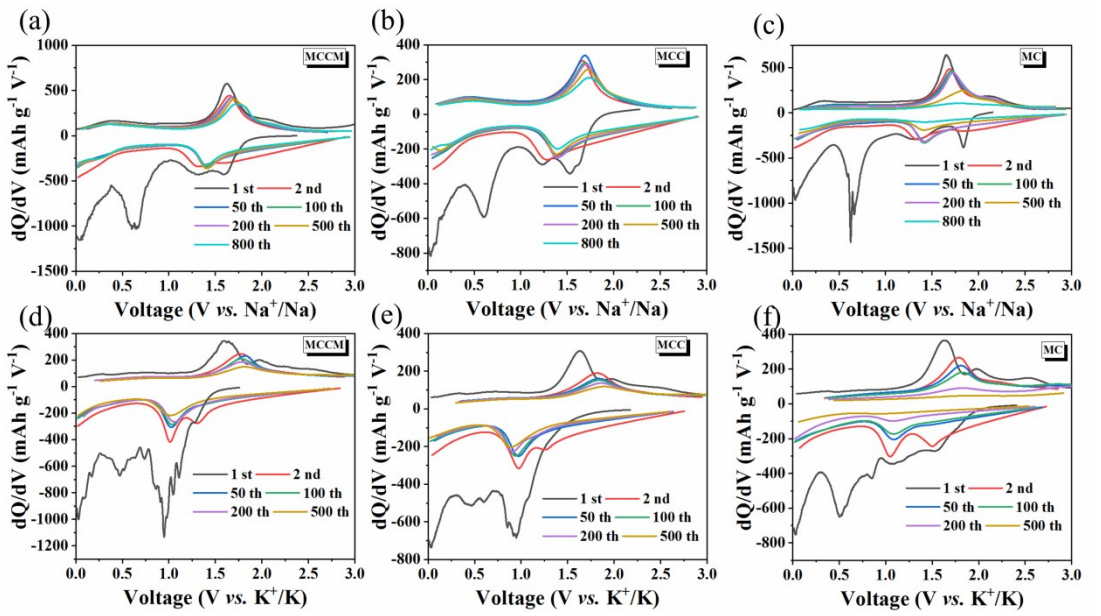

Fig. S7. The d*Q*/d*V* curves transformed from the selected discharge/charge profiles for the (a-c)

SIBs and (d-f) PIBs at 1.0 A g^{-1} (0.05 A g^{-1} for the initial cycle) for the MC, MCC and MCCM samples.

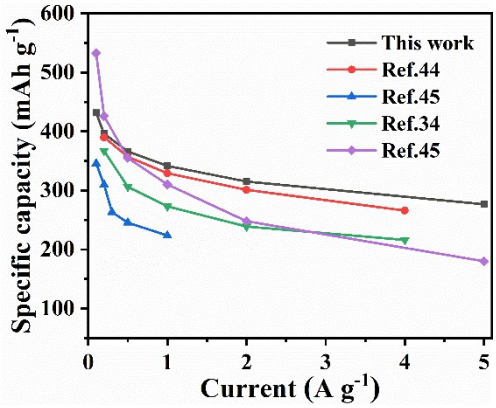

Fig. S8. Comparison of the sodium storage performances between this work and the some reported $MoSe_2$-based anodes.

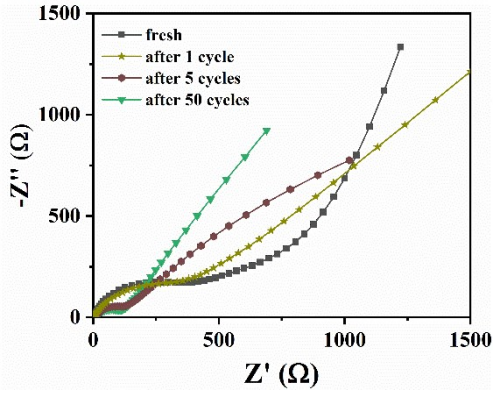

Fig. S9. Nyquist plots of fully charged cells after different cycles.

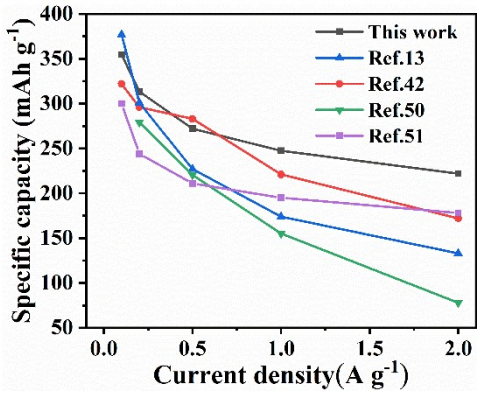

Fig. S10. Comparison of the potassium storage performances between this work and some

reported $MoSe_2$-based anodes.

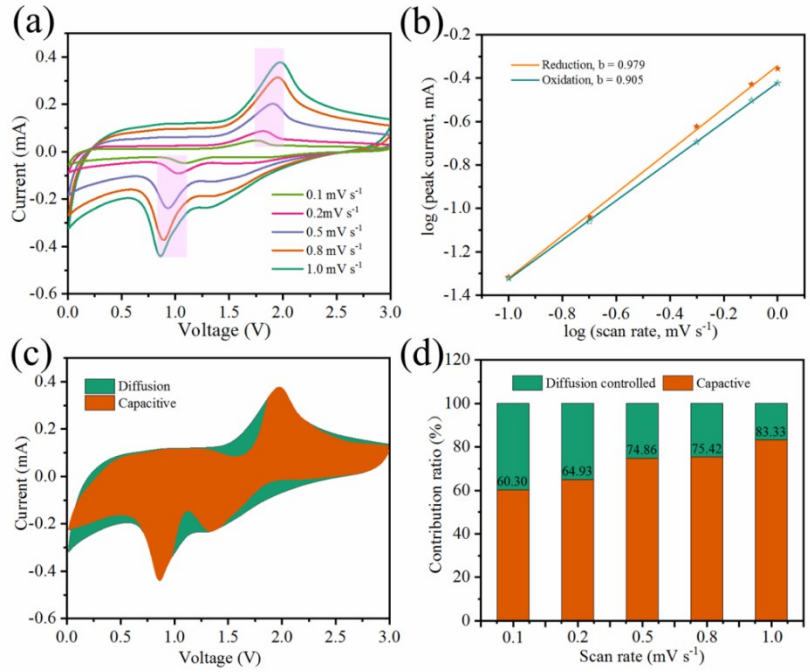

Fig. S11. Kinetics analysis of the K^+-ion storage behavior. (a) CV curves with varying scan rates, (b) *b*-value analysis based on the relationship between the peak currents and the scan rates, (c) capacitive and diffusion-controlled charge storage separation for the CV curve at 0.1 mV s^{-1}, (d) contribution ratio of the capacitive and diffusion-controlled charges at different scan rates for the MCCM anode.

The kinetics analysis of the K^+-ion storage is performed through capacity contribution analysis, as shown in Fig. R8. Similar to the SIBs, CV of PIBs scans ranging from 0.1 to 1.0 mV s^{-1}, exhibit similar redox peaks, except for the peak shifting and intensity variation, as shown in Fig. S11a. The b values of cathodic and anodic peaks are inferred to be 0.979 and 0.905 (Fig. S11b), implying that the fast reaction kinetics is mainly promoted by pseudocapacitive behavior. As illustrated in Fig. S11c, the capacitive contribution of MCCM is calculated to be 60.3% at 0.1 mV s^{-1}. Along with the scan rates increase, the capacitive contribution to the total capacity gradually increases, and can reach 83.33% at scan rate of 1.0 mV s^{-1} (Fig. S11d), which further proves the

fast electrochemical reaction kinetics is mainly promoted by the capacitive contribution.